Nonlinear modal coupling in a high-stress doubly-clamped nanomechanical resonator

2012 New J. Phys. 14 113040

(http://iopscience.iop.org/1367-2630/14/11/113040)

New Journal of Physics
The open access journal for physics

Nonlinear modal coupling in a high-stress doubly-clamped nanomechanical resonator

K J Lulla[1], R B Cousins, A Venkatesan[2], M J Patton, A D Armour, C J Mellor and J R Owers-Bradley[3]

School of Physics and Astronomy, University of Nottingham, Nottingham NG7 2RD, UK
E-mail: john.owers-bradley@nottingham.ac.uk

New Journal of Physics **14** (2012) 113040 (14pp)
Received 3 May 2012
Published 28 November 2012
Online at http://www.njp.org/
doi:10.1088/1367-2630/14/11/113040

Abstract. We present results from a study of the nonlinear inter-modal coupling between different flexural vibrational modes of a single high-stress, doubly-clamped silicon nitride nanomechanical beam. Using the magnetomotive technique and working at 100 mK we explored the nonlinear behaviour and modal couplings of the first, third and fifth modes of a 25.5 μm long beam. We find very good agreement between our results and a simple analytical model which assumes that the different modes of the resonator are coupled to each other by displacement induced tension in the beam. The small size of our resonator leads to relatively strong nonlinear couplings, for example we find a shift of about 7 Hz in the third mode for a 1 nm displacement in the first mode and frequency shifts ~20 times larger than the linewidth (130 Hz) are readily observed.

[1] Current address: Institut Néel, CNRS and Université Joseph Fourier, BP 166, F-38042 Grenoble Cedex 9, France.
[2] Current address: IISER, Mohali, Knowledge City, Sector 81, SAS Nagar, Manauli, PO Box 140306, India.
[3] Author to whom any correspondence should be addressed.

Contents

1. Introduction

Nonlinear effects are a common feature in experiments on nanoelectromechanical systems (NEMS) [1–12]. From a practical point of view, nonlinearities need to be understood because of their impact on applications of NEMS as sensors [4, 13, 14]. However, the very high operating frequencies of NEMS devices (which are typically in the MHz range), and the ease with which the nonlinear regime can be reached, make them ideal for investigating fundamental aspects of nonlinear dynamics [5, 7–10, 12]. Furthermore, following recent progress in which experiments on nanomechanical resonators reached the quantum regime [15–17], nonlinear effects are expected to play a key role in future work as they are predicted to give rise to important signatures of the transition from classical to quantum regimes [18] as well as providing tools for quantum measurements [19].

Nonlinearities in NEMS devices typically lead to Duffing-type behaviour in the response of a single mode, though damping can also be affected [2, 20]. However, recent experiments have highlighted the importance of the couplings between different mechanical modes within a single beam [10, 11, 21] or cantilever [22] that can be generated in the nonlinear regime. Interest in nonlinear modal couplings has been stimulated by progress in optomechanical systems [15, 16] which are engineered to have strong couplings between optical and mechanical modes. The coupling to a high frequency optical [16] (or microwave [15]) mode which is strongly driven slightly off resonance provides a very effective way of manipulating the state of a mechanical mode and such systems have indeed been used to cool a mechanical mode with frequency as low as 10 MHz into almost the quantum ground state [15, 16]. Experiments have begun to investigate the question of whether inter-modal couplings in mechanical resonators can be exploited in an analogous way with a higher frequency mechanical mode driven at an appropriate frequency being used to change the Q-factor of a lower frequency mode in the same resonator [21, 22] or even, possibly, to cool it [21].

In this work we focus on understanding in precise detail the underlying mechanism that gives rise to modal couplings in nanomechanical beam resonators under high intrinsic stress. We present a systematic study of the nonlinear response of three of the flexural modes of a nanomechanical beam resonator, together with the associated inter-mode couplings. We report the results of a series of measurements taken at 100 mK on the fundamental, third and fifth harmonics (all of which are in the MHz range) of a doubly-clamped beam fabricated from high-stress ($\sim$1 GPa) silicon nitride. In a first set of measurements, we excite one mode at a time and find that they display a Duffing-like behaviour which can be understood quite naturally in terms of the nonlinearity arising from the stretching of the beam that accompanies

its bending [2]. We then measure the response when two modes are driven at the same time, with one mode acting as a probe of the displacement of the other. The high tensile stress and the low temperature mean that the Q-factor of the modes is high enough [23] to allow us to observe the higher mode resonance signals as well as the frequency shifts induced by nonlinear mode–mode couplings which are much larger than the linewidth. Using the single-mode results to calibrate our measuring scheme we are able to make a detailed quantitative comparison (without the need for any fitting parameters) between our coupled-mode results and the predictions of a simple model of the stretching nonlinearity. Our study builds on recent work by Westra *et al* [10] which showed that the stretching nonlinearity could account for nonlinear coupling between the first and third harmonics of a micromechanical doubly-clamped beam. However, our experiments explore a regime which is quite different to that investigated by Westra *et al* [10] and which, given the MHz frequencies of our device and the low temperatures, is much closer to the conditions where quantum effects are likely to become important[4].

This paper is organized as follows. Section 2 introduces a simple theoretical model of the stretching nonlinearity in beam resonators. The experimental set-up is outlined in section 3 and in section 4 we describe our results. We give our conclusions in section 5.

2. Theoretical background

Here we review the theoretical description of a beam under tension [24], starting from the Euler–Bernoulli equation extended to include the geometric nonlinearity arising from the stretching of the beam that accompanies its flexure [2, 25]. For a single mode, this nonlinearity leads naturally to the Duffing equation where a term proportional to the cube of the displacement is added to the usual harmonic equation of motion [2]. However, the nonlinearity also generates important couplings between different modes [10].

We start by considering a doubly-clamped beam of length L, lying along the x-axis, with cross-sectional area $A = wh$, where here w is the dimension in the direction of motion and h the dimension perpendicular to the motion. The beam is assumed to be under intrinsic tension, T_0, and we include, to lowest order, the nonlinear tension arising from the stretching of the beam [2]. The equation of motion for the displacement, y, is given by

$$\rho A\ddot{y} + \eta\dot{y} + EI_y y'''' - \left[T_0 + \frac{EA}{2L}\int_0^L (y')^2\,\mathrm{d}x\right] y'' = F_L, \tag{1}$$

where ρ is the density, η characterizes the damping, $I_y = hw^3/12$ is the moment of inertia, F_L is the force per unit length exerted on the beam and E the Young's modulus. The nonlinearity arises from the second term within the square brackets.

The mode frequencies and mode functions for the corresponding linear problem are known [24] and provide a convenient starting point for describing the nonlinear regime. If the system is driven harmonically, $F_L = F_n\cos(\omega_n t)$, at a frequency close to one of the linear mode frequencies $\omega_{n,0}$, we can then approximate the displacement of the beam as $y(x,t) = wg_n(x)u_n(t)$ where $g_n(x)$ is the nth mode function, normalized so that $\int_0^1 g_n^2(\tilde{x})\,\mathrm{d}\tilde{x} = 1$ where $\tilde{x} = x/L$.

[4] The mechanical resonator used in [10] was much larger (length ~1 mm) and without intrinsic tension; the mode frequencies were in the kHz range with Q-factors $\simeq 10^2$ and the experiments were conducted at room temperature.

The dimensionless function $u_n(t)$ obeys the equation of motion [2]

$$\frac{\mathrm{d}^2u_n}{\mathrm{d}t^2}+\frac{\omega_{n,0}}{Q_n}\frac{\mathrm{d}u_n}{\mathrm{d}t}+\omega_{n,0}^2u_n+\lambda I_{nn}^2u_n^3=f_n\cos(\omega_n t), \tag{2}$$

where $\lambda=(Ew^2)/(2\rho L^4)$, $f_n=F_n\xi_n/(hw^2\rho)$, with $\xi_n=\int_0^1 \mathrm{d}\tilde{x}\,g_n(\tilde{x})$ (the mode parameter), and the Q-factor of the nth mode is given by $Q_n=\omega_{n,0}(A\rho/\eta)$. Of particular note is the strong dependence on length of the coupling parameter, λ, which tells us that the coupling will increase rapidly with decreasing resonator length (note that λ, depends on w^2 because we have chosen to scale the physical displacement, y by w to obtain the amplitude u). The strength of the nonlinearity is also controlled by the parameter I_{nn} which is defined by an integral of the form, $I_{ij}=\int_0^1 \mathrm{d}\tilde{x}\,g_i'(\tilde{x})g_j'(\tilde{x})$ (with i and j labelling any two modes of the beam).

Since the equation of motion (equation (2)) is that of the familiar Duffing oscillator, we proceed to analyse it using standard methods [26]. Substituting a solution of the form

$$u_n=a_n\cos(\omega_n t)+b_n\sin(\omega_n t), \tag{3}$$

into equation (2), we obtain an equation for the amplitude of the motion, $r_n=(a_n^2+b_n^2)^{1/2}$,

$$r_n=f_n\left[\left(\omega_{n,0}^2+\frac{3}{4}\lambda I_{nn}^2r_n^2-\omega_n^2\right)^2+\left(\frac{\omega_n\omega_{n,0}}{Q_n}\right)^2\right]^{-1/2}. \tag{4}$$

For a large enough quality factor, Q_n, and for relatively small amplitudes, r_n, the main effect of the nonlinearity is to shift the frequency of peak response to

$$\omega_{n,1}=\omega_{n,0}\sqrt{1+\frac{3\lambda I_{nn}^2}{4\omega_{n,0}^2}r_n^2}. \tag{5}$$

In the weakly nonlinear regime, the frequency of the resonator shifts from its natural (undriven) value quadratically with increasing amplitude (frequency pulling) [25, 26].

We now consider a situation where the drive contains two harmonic components

$$F_L=F_n\cos(\omega_n t)+F_m\cos(\omega_m t), \tag{6}$$

with the two drives frequencies ω_n and ω_m chosen to be close to the resonant frequencies of two different modes, $\omega_{n,0}$ and $\omega_{m,0}$, respectively. In this case we assume the beam displacement can be approximated as, $y(x,t)=w[u_n(t)g_n(x)+u_m(t)g_m(x)]$.

Following the same approach as for the one mode case, assuming u_n and u_m each oscillate at a single frequency (i.e. they take the form of equation (3)), we obtain a modified expression for the amplitude of mode n

$$r_n=f_n\left[\left(\omega_{n,2}^2-\omega_n^2\right)^2+\left(\frac{\omega_n\omega_{n,0}}{Q_n}\right)^2\right]^{-1/2}, \tag{7}$$

where

$$\omega_{n,2}=\omega_{n,0}\sqrt{1+\frac{3\lambda I_{nn}^2}{4\omega_{n,0}^2}r_n^2+\frac{\lambda}{\omega_{n,0}^2}\left(\frac{1}{2}I_{nn}I_{mm}+I_{nm}^2\right)r_m^2}. \tag{8}$$

Thus we see that the frequency of a given mode depends not just on the amplitude of its own motion, but the amplitude of the other mode that is excited. In particular, the frequency shift of one mode initially grows quadratically with the amplitude of the other one.

3. Experimental set-up

Experiments were performed on a silicon nitride beam with length 25.5 μm, width 170 nm and thickness 170 nm. Metal layers consisting of 3 nm of Ti and 40 nm of Au were added by thermal deposition to form a wire on top of the beam through which a drive current could be applied. The devices were fabricated by dry-etching in a multi-stage process [27] from wafers composed of a 190 μm thick silicon wafer with 170 nm of silicon nitride on both sides; the nitride layer has a built-in tensile stress of about 1070 MPa at room temperature[5]. The beam was excited in such a way that its motion was parallel to the plane of the surrounding substrate (along the y-axis in figure 1(a)) and hence the dimension in the direction of flexure was the width w.

A schematic diagram of the experimental set-up is shown in figure 1(a). The resonator was placed inside a ^{3}He/^{4}He dilution refrigerator and measurements were performed at 100 mK. The motion of the beam was monitored using the magnetomotive method [28]. A magnetic field of $B = 3$ T was applied and the drive was applied by passing an alternating current through the sample. The response to the resulting Lorentz force was detected by measuring a voltage (V_a), which is related to the input voltage at the rf pre-amplifier (V_0), as the frequency of the drive signal was tuned through the mechanical resonance. The beam was driven at two different frequencies by using an additional signal generator as shown in figure 1(a). The measurements were carried out in transmission mode, see figure 1(b), capturing a dip in the conductance of the beam in the spectral domain.

The motion of the resonator in the magnetic field generates an electromotive force (emf) [28], which itself is related to the mechanical motion. Provided that the resonances are well-resolved, $|\omega_{m,0} - \omega_{n,0}| \gg \frac{\omega_{m,0}}{Q_m} + \frac{\omega_{n,0}}{Q_n}$, for $m \neq n$, the motion at a given frequency can be attributed to a single mode and

$$V_{\rm emf} = w\xi_n L B \frac{\partial u_n}{\partial t}. \tag{9}$$

We can relate the final measured voltage, V_{an} to $V_{\rm emf}$, and hence to the amplitude of a given mode, r_n, by applying Kirchoff's law to the circuit (figure 1(b)) and solving the corresponding equations. Thus we find

$$V_{an} = GV_0 = \frac{Z_0 G}{Z_0 + Z_{\rm e}} \left(V_{\rm in} - V_{\rm emf}\right), \tag{10}$$

where G is a constant of proportionality that quantifies the overall signal gain from the sample to the network analyser, taking into account the losses in the transmission cables as well as the gain provided by the amplifiers. The gain in the transmission line will in fact vary slightly with frequency (hence the gain will not be the same for different modes) and local temperature variations inside the fridge. Mechanical resonance leads to a dip in the voltage V_{an}, hence (assuming the circuit impedances are real) we can characterize the mechanical response of a particular mode by

$$\begin{aligned} V_{Sn} &= \left| \frac{Z_0 G}{Z_0 + Z_{\rm e}} V_{\rm in} - V_{an} \right| \\ &= \frac{Z_0}{Z_0 + Z_{\rm e}} G B L w \xi_n \omega_n r_n, \end{aligned} \tag{11}$$

[5] The silicon nitride layers were deposited on the silicon substrates using a low pressure chemical vapour deposition process at the Cornell Nanoscale Science and Technology Facility (CNF), 250 Duffield Hall, Cornell University, Ithaca, NY, USA.

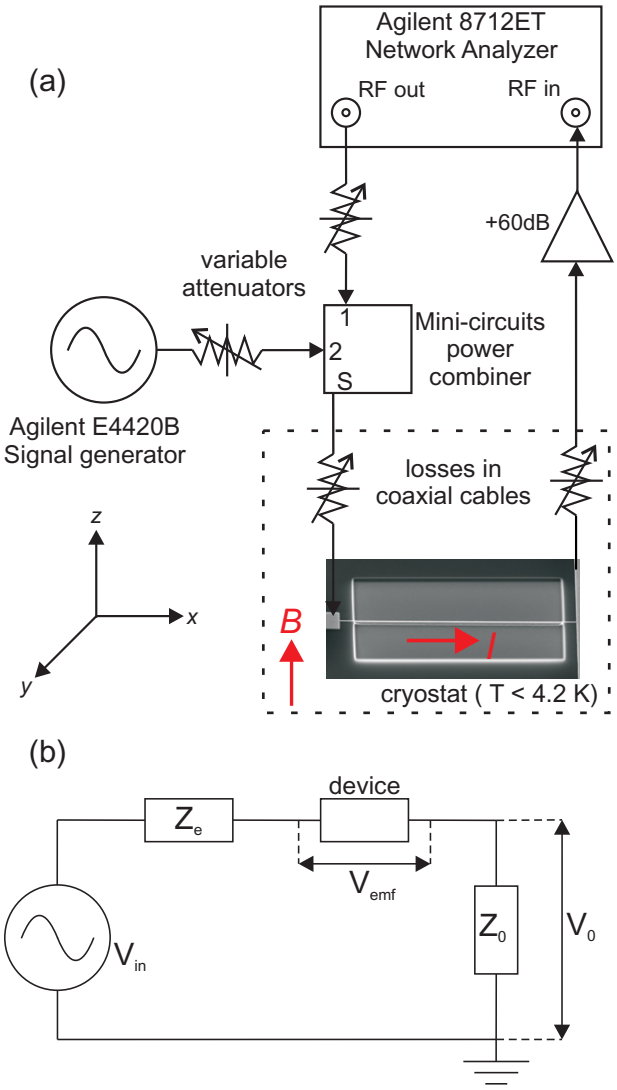

Figure 1. (a) Schematic diagram of the measurement set-up. The different modes of the beam were driven with two separate signal generators. A voltage signal which depends on the (emf) generated by the beam was detected at the input of the network analyser after passing through a pre-amplifier. (b) Circuit model for transmission measurements, with external circuit impedances Z_e and Z_0, the drive voltage V_{in}, the emf generated by the device, V_{emf}, and the measured voltage V_0.

which measures the size of the dip. Expanding equation (5) to lowest order in r_n and using equation (11) leads to the explicit expression

$$\omega_{n,1} = \omega_{n,0} + \alpha_n V_{Sn}^2, \tag{12}$$

where $\alpha_n = \frac{3I_{nn}^2 \lambda \omega_{n,0} D_n}{8(BL\omega_n \xi w)^2}$ and $D_n = \left(\frac{Z_0+Z_e}{Z_0}\frac{1}{G}\right)^2$.

Table 1. Properties of the three measured modes of the silicon nitride beam.

n	$\omega_{n,0}/2\pi$ (MHz)	ξ_n	I_{nn}	Q_n
1	7.50	0.88	10.4	9.0×10^3
3	22.85	0.30	93.3	1.7×10^5
5	39.28	0.19	257.9	4.1×10^5

4. Results

We were able to detect the first three odd harmonics of the beam which had frequencies 7.5, 22.85 and 39.28 MHz, respectively (the even modes do not give rise to a signal which is directly measurable using the magnetomotive method). Measurements on each individual mode were performed first, capturing the response of the resonator as the driving frequency was swept through the mechanical resonant frequency. The basic properties of the three modes are summarized in table 1. The frequencies are those measured at the lowest drive levels used. The Q-factors are the measured values at a field of 3 T. Although the values are still rather high, the relatively strong magnetic field used means that they are lower than the intrinsic Q-factors of the modes [28, 29] (much lower in the case of the $n = 1$ mode [27] whose intrinsic Q-factor is 1.8×10^6 at 100 mK).

The nonlinear parameters, I_{nn}, and the mode parameters, ξ_n, are calculated numerically using a value of the intrinsic stress, which we estimate to be $T_0/A = 1020$ MPa. This is slightly lower than the room temperature value because of the different thermal contractions of the silicon and silicon nitride layers in the wafer [27]. The parameters, I_{nn}, and hence the strength of the nonlinearity in a given mode, grow rapidly in size with the mode number n. The cross terms, I_{nm}, which involve two different modes, also grow with the mode number, but are much smaller for our device: $I_{13} = -1.9$, $I_{15} = -3.0$ and $I_{35} = -8.8$. In calculating the parameter $\lambda = (Ew^2)/(2\rho L^4)$ we use the Young's modulus of silicon nitride [30], $E_{\mathrm{SiN}} = 211$ GPa and neglect the contribution from the gold as it is under much less tension and its Young's modulus, $E_{\mathrm{Au}} = 78$ GPa, is smaller. We include the effect of the gold layer on the mass by using an appropriate average value for the density. Using these parameters we obtain theoretical estimates of the three mode frequencies of 7.8, 24.2 and 42.5 MHz, respectively, which are all close to the measured values (given in table 1). The discrepancies between estimated and measured frequencies arise from the uncertainties in the device dimensions ($L \sim \pm 1\%$, $w \sim \pm 5\%$ and $t_{\mathrm{Au}} \sim \pm 10\%$).

Data were collected for a range of drive amplitudes by systematically increasing the drive signal. As an example, the spectral response of the fundamental mode is shown in figure 2 as a function of the corresponding drive amplitude. As expected, the curves are symmetric for the smallest drives, but become increasingly asymmetric as the beam is driven harder. At the largest amplitudes, the device enters a strongly nonlinear regime marked by sharp changes seen in the measured signal on the high frequency side of the resonance[6]. Frequency pulling is also clearly visible, with the peak frequency of each mode shifting upwards as the drive is increased. Very similar behaviour is seen for modes 3 and 5.

We extracted the frequencies of peak response, $f_{n,1} = \omega_{n,1}/2\pi$ and the corresponding voltages V_{Sn} from the measured resonance curves (figure 2). The shift in peak frequency,

[6] Note that when these measurements were taken the frequency was always swept upwards.

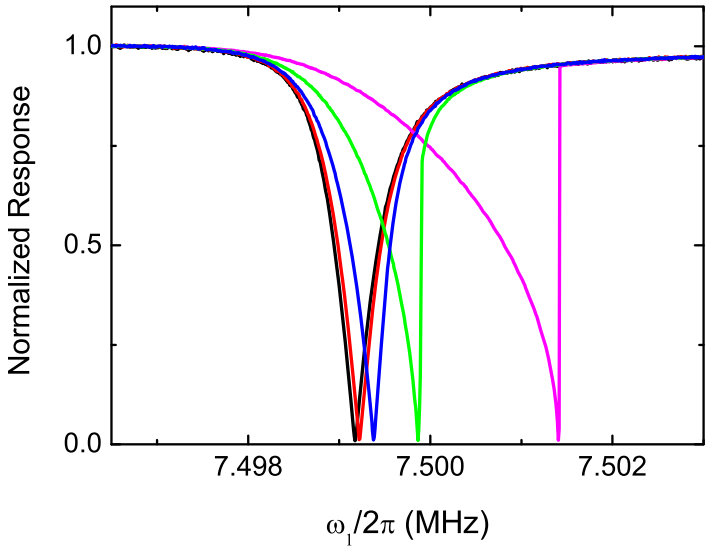

Figure 2. Resonant response of mode 1 (7.5 MHz). The curves from left to right correspond to a series of increasing drive strengths. The normalized response consists of the measured voltage, V_{a1}, scaled by the maximum value measured in each case.

$\Delta f_{n,1} = (\omega_{n,1} - \omega_{n,0})/2\pi$, versus peak measured voltage V_{Sn}, for each mode is shown in figure 3. Theory predicts (see equation (12)) that the frequency shift should increase quadratically with the voltage and this is what is found. All the parameters required for the analysis are known (with stated uncertainty) except for the D_n. We obtain a value of the quadratic coefficient, α_n, for each mode by fitting each set of measured data to a quadratic function with a fitting error of less than 3%, from which we then calculate the D_n. The fits are shown as lines in figure 3. The value of D_n varies between the modes by about a factor of two, due to the intrinsic frequency dependence of the circuit impedances and amplifier gain. The error in D_n is about 13% and follows directly from the error in sample dimensions.

Next we probed the interactions between the different modes of the beam by exciting one mode weakly and measuring its response as successively stronger drive amplitudes (of a fixed frequency) were applied to a second mode. The shift in the peak response frequency of the weakly driven mode, $\Delta f_{n,2} = (\omega_{n,2} - \omega_{n,0})/2\pi$, was measured together with the voltage at the frequency of the strongly driven mode. Response curves for mode 3, measured for three different levels of drive applied to mode 1, is shown in figure 4. As expected, the resonant frequency of mode 3 increases with the measured voltage from the first mode. Looking at the depths of the curves in figure 4, we see that increasing the amplitude of the mode 1 drive reduces the amplitude of the response of mode 3 slightly [10]. A reduction in the peak amplitude is a natural consequence of an increase in the frequency $\omega_{n,2}$ (see equation (7)), but we also find a very slight degradation in the Q-factor of the third mode accompanies the increasing drive at the fundamental frequency.

The shift in the peak response frequencies of the third and fifth modes as a function of the voltage measured at the frequency of mode 1, V_{S1}, are shown in figure 5. Similarly, figure 6 shows the effect of varying the amplitude of the third mode on the resonant frequency of the first and fifth modes. Again the theory predicts (through equations (8) and (11)) a quadratic

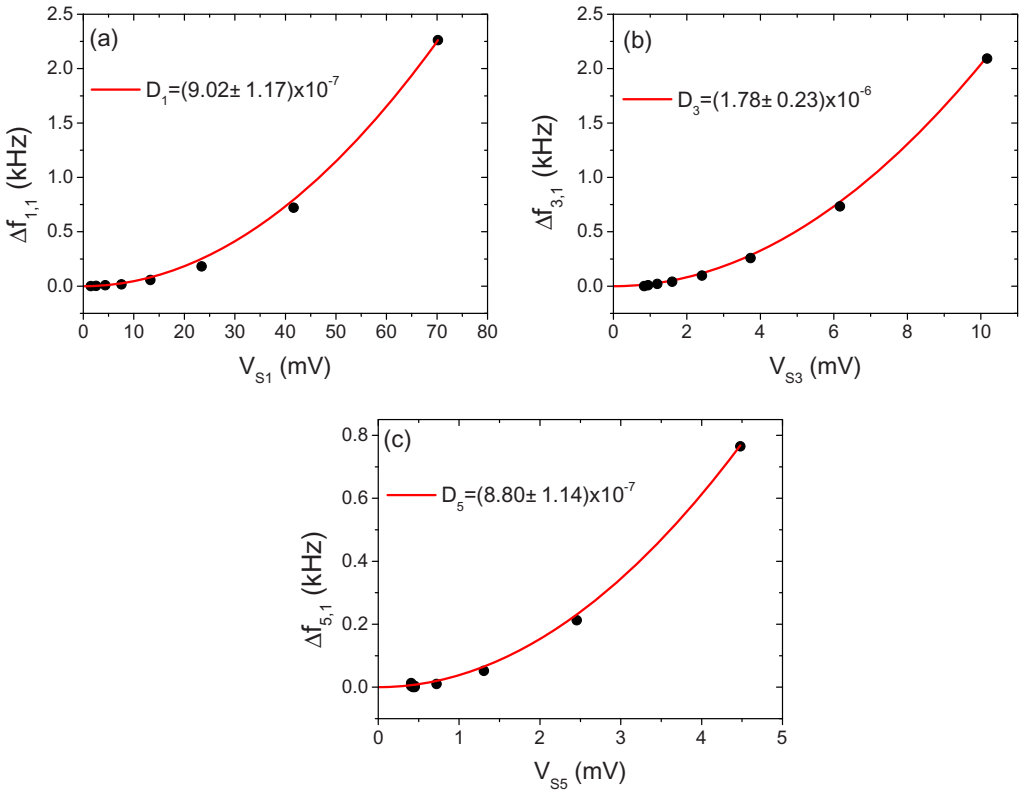

Figure 3. Shift in the frequency, $\Delta f_{n,1}$, as a function of the voltage V_{Sn} for (a) $n = 1$, (b) $n = 3$ and (c) $n = 5$. The points are the data and the lines are quadratic fits. The corresponding values of the parameters D_n obtained from the fit, together with the associated uncertainty, are given in each case.

dependence of the frequency shifts on the measured voltages. However, because the values of the parameters α_n have been determined from fits to the single-mode data, the comparison with theory now involves no free parameters. We use the α_n values extracted from the single mode data, and the parameters I_{nm}, together with the associated uncertainties, to plot shaded bands in figures 5 and 6 showing the regions which are fully consistent with the theory. We note that the I_{nm} values are quite insensitive to the changes in beam dimensions, so the predictions of the theory are fairly precise. In each case it is clear that the dependence of the frequency shifts on the voltages is well described by a quadratic law, and that there is very good agreement between the theoretical predictions and the measurements.

Having verified that the bending nonlinearity provides a quantitatively accurate description of the modal couplings in the beam, we can now obtain the amplitude of the motion in one mode by measuring the frequency shifts in a second (weakly driven) mode. The theoretical expression, equation (8), and the mode function $g_n(x)$ allow us to convert from a measured frequency shift to a physical amplitude at a given point along the beam. An example is shown in figure 7 in which the amplitude of mode 1 at the antinode $x = L/2$, obtained by measuring a frequency shift in mode 3, is shown as a function of the drive frequency, ω_1. An amplitude of 1 nm in mode 1 translates into a frequency shift in mode 3 of 7.11 Hz. From figure 7 we see that an amplitude of 25 nm ($\sim$10% of the width of the beam) is already well within the nonlinear regime.

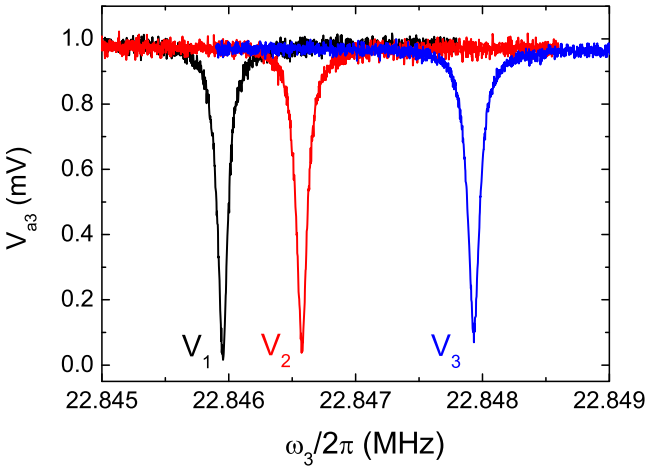

Figure 4. Response curves of the third flexural mode for different measured voltages, V_{S1}, at the frequency of the first mode, $V_1 = 15.2\,\mathrm{mV}$, $V_2 = 29.3\,\mathrm{mV}$ and $V_3 = 48\,\mathrm{mV}$, corresponding to three successively increasing drive amplitudes applied at a fixed frequency of 7.499 MHz.

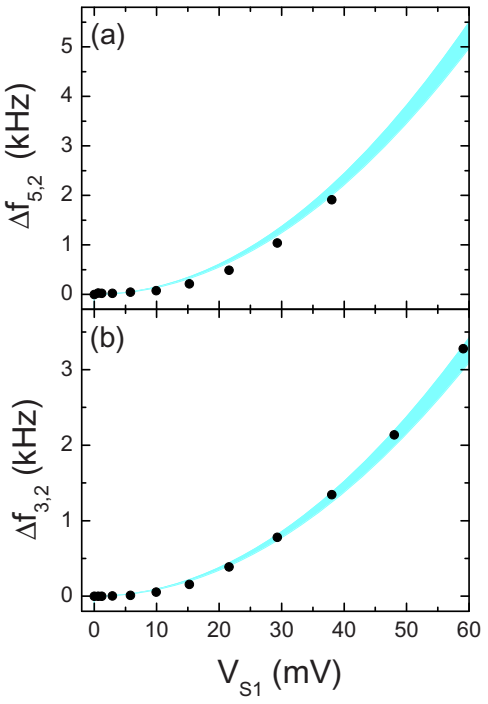

Figure 5. Frequency shifts of (a) the fifth mode, $\Delta f_{5,2}$, and (b) the third mode $\Delta f_{3,2}$, as a function of the measured response of the first mode, V_{S1}, to a sequence of progressively stronger drives. In each case the points are data, and the shaded area is the band of values consistent with theoretical predictions when uncertainties in the parameters are accounted for.

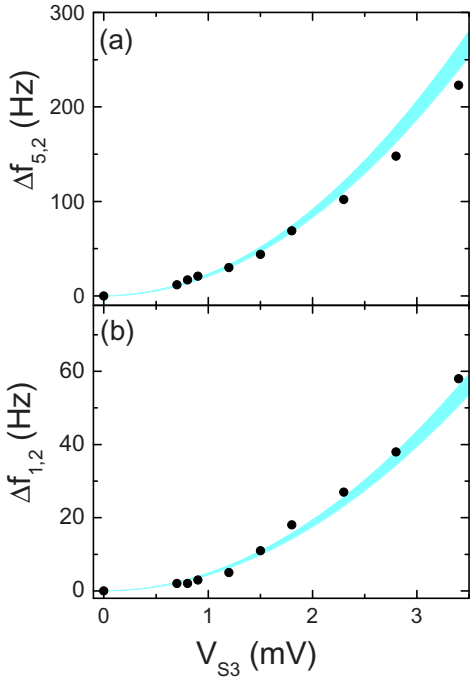

Figure 6. Frequency shifts of (a) the fifth mode, $\Delta f_{5,2}$, and (b) the first mode $\Delta f_{1,2}$, as a function of the measured response of the third mode, V_{S3}, to a sequence of progressively stronger drives. In each case the points are data, and the shaded area is the band of values consistent with theoretical predictions when uncertainties in the parameters are accounted for.

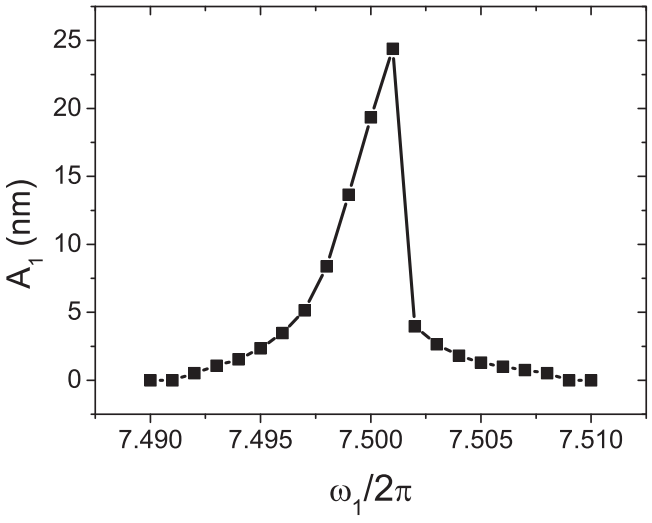

Figure 7. Amplitude of the motion of mode 1 (at the antinode), A_1, as a function of the drive frequency $\omega_1/2\pi$ obtained using the frequency shift in mode 3. Each point is generated by measuring a full frequency response curve for mode 3 from which the resulting $\Delta f_{3,2}$ is obtained and then converted into an amplitude for mode 1.

5. Conclusions

We have measured the properties of three of the flexural modes of a highly stressed, doubly-clamped silicon nitride nanomechanical beam. The size of the sample, the Q-factors, the temperature and the degree of nonlinearity are all orders of magnitude different than reported by Westra *et al* [10] for an unstressed beam at room temperature. As a first step we investigated the frequency pulling that accompanies increases in the drive applied to each of the modes in turn. For all three modes the frequency was found to grow quadratically with the amplitude of the motion, consistent with the Duffing-type behaviour predicted for a nonlinearity governed by the stretching of the beam on deflection.

We then examined the behaviour of the system when one mode is driven weakly and the amplitude of the drive applied to a second mode is increased steadily. We again found that the frequency of the weakly driven mode increased quadratically, this time with the amplitude of the second mode. Using the results from the single-mode experiments to calibrate our measurement set-up we were able to make a comparison without any free parameters to theoretical predictions. The good agreement we find using four different pairs of modes allows us to conclude that the nonlinear dynamics we observe does indeed arise from the stretching of the beam on deflection. Our data confirm that the bending nonlinearity provides a good quantitative description of the mode couplings in our nanomechanical device.

An interesting comparison can be made with the results obtained using a micromechanical resonator described in [10]. The frequency shift we observe in the third mode due to a 1 nm displacement of the first mode is a factor of $\sim 3 \times 10^4$ larger[7] than that observed in [10]. This difference is largely due to the much smaller dimensions of our device, and in particular its length, which is a factor of 40 smaller than that used in [10], as the nonlinear coupling strength is strongly dependent on the length of the beam (as noted in section 2). In contrast to [10] our device is under high tension and is in fact close to the stretched string limit. However, this does not significantly affect the strength of the nonlinear coupling as although some of the nonlinear parameters (i.e. the cross terms I_{nm} where $n \neq m$) are strongly suppressed in the high-tension limit, those nonlinear parameters which dominate the mode–mode coupling (the terms I_{nn}) are only slightly affected by the tension [10, 31]. On the other hand, the high tension in our device, combined with our use of low temperatures, leads to much higher Q-factors than those achieved in the experiments on micromechanical resonators (for example the Q-factor of our third mode is larger by about a factor of 10^3 than that in [10]) which in turn facilitates our measurements of the fifth mode and its interactions in addition to the first and third modes. The high Q-factors of the modes also greatly improves the overall ability to resolve small displacements in one mode via their effect on the frequency of another mode as it is the frequency shift in relation to the underlying linewidth which sets a limit on sensitivity. The frequency shifts we observe are often much larger than the corresponding linewidths (in contrast to the shifts seen in [10] which are at most a fraction of the linewidth).

The finding that frequency shifts much larger than the linewidth can be induced in the third and fifth harmonics by the fundamental mode and vice versa in our nanomechanical device has very positive implications for attempts to improve on the recent experiments which sought to emulate the effects (such as cooling) achieved in optomechanical systems [21, 22]. If effective optomechanical cooling is to be achieved using inter-modal couplings then it will be necessary to use couplings between modes which are widely separated in frequency so that one of them has

[7] Our comparison is made with the quadratic curve shown in figure 1(c) of [10].

a much lower thermal occupation than the other [21]. Thus an important goal for future work will be to explore just how far up into the higher harmonics one can detect frequency shifts due to motion at the fundamental frequency. However, the fact that each of the mechanical modes also has a Duffing nonlinearity that affects its dynamics at rather small amplitudes is an important difference from a conventional optomechanical system where nonlinearity in the optical mode does not normally need to be considered [32].

Acknowledgments

We thank E Collin for helpful discussions and acknowledge financial support from EPSRC (UK) under grant no. EP/E03442X/1.

Note Added in Proof. Since this work was submitted two related works which investigate modal coupling in carbon nanotube resonators have been published [33, 34].

References

[1] Blick R H *et al* 2002 *J. Phys.: Condens. Matter* **79** 905
[2] Lifshitz R and Cross M C 2008 *Reviews of Nonlinear Dynamics and Complexity* ed H G Schuster (Weinheim: Wiley) chapter 1, p 52
[3] Rhoads J F, Shaw S W and Turner K L 2010 *J. Dyn. Syst. Meas. Control* **132** 034001
[4] Postma H W Ch, Kozinsky I, Husain A and Roukes M L 2005 *Appl. Phys. Lett.* **86** 223105
[5] Aldridge J S and Cleland A N 2005 *Phys. Rev. Lett.* **94** 156403
[6] Kozinsky I, Postma H W Ch, Bargatin I and Roukes M L 2006 *Appl. Phys. Lett.* **88** 253101
[7] Almog R, Zaitsev S, Shtempluck O and Buks E 2006 *Appl. Phys. Lett.* **88** 213509
[8] Kozinsky I, Postma H W Ch, Kogan O, Husain A and Roukes M L 2007 *Phys. Rev. Lett.* **99** 207201
[9] Karabalin R B, Cross M C and Roukes M L 2009 *Phys. Rev.* B **79** 165309
[10] Westra H J R, Poot M, van der Zant H S J and Venstra W J 2010 *Phys. Rev. Lett.* **105** 117205
[11] Dunn T, Wenzler J-S and Mohanty P 2010 *Appl. Phys. Lett.* **97** 123109
[12] Collin E, Bunkov Yu M and Godfrin H 2010 *Phys. Rev.* B **82** 235416
[13] Ekinci K L and Roukes M L 2005 *Rev. Sci. Instrum.* **76** 061101
[14] Guerra D N, Bulsara A R, Ditto W L, Sinha S, Murali K and Mohanty P 2010 *Nano Lett.* **10** 1168
[15] Teufel J D, Donner T, Li D, Harlow J W, Allman M S, Cicak K, Sirois A J, Whittaker J D, Lehnert K W and Simmonds R W 2011 *Nature* **475** 359
[16] Chan J, Mayer Alegre T P, Safavi-Naeini A H, Hill J T, Krause A, Gröblacher S, Aspelmeyer M and Painter M 2011 *Nature* **478** 89
[17] Poot M and van der Zant Herre S J 2012 *Phys. Rep.* **511** 273
[18] Katz I, Retzker A, Straub R and Lifshitz R 2007 *Phys. Rev. Lett.* **99** 040404
[19] Santamore D H, Doherty A C and Cross M C 2004 *Phys. Rev.* B **70** 144301
[20] Eichler A, Moser J, Chaste J, Zdrojek M, Wilson-Rae I and Bachtold A 2011 *Nature Nanotechnol.* **6** 339
[21] Mahboob I, Nishiguchi K, Okamato H and Yamaguchi H 2012 *Nature Phys.* **8** 387
[22] Venstra W J, Westra H J R and van der Zant H S J 2011 *Appl. Phys. Lett.* **99** 151904
[23] Verbridge S S, Finkelstein-Shapiro D, Craighead H G and Parpia J M 2007 *Nano Lett.* **7** 1728
[24] Bokaian A 1990 *J. Sound Vib.* **142** 481
[25] Nayfeh A H and Mook D T 1979 *Nonlinear Oscillations* (New York: Wiley)
[26] Hand L N and Finch J D 1998 *Analytical Mechanics* (Cambridge: Cambridge University Press)
[27] Lulla K 2011 *PhD Thesis* University of Nottingham
[28] Cleland A N and Roukes M L 1999 *Sensors Actuators* A **72** 256

[29] Venkatesan A, Lulla K J, Patton M J, Armour A D, Mellor C J and Owers-Bradley J R 2010 *Phys. Rev.* B **81** 073410
[30] Chuang W-H 2004 *J. Microelectromech. Syst.* **13** 870
[31] Poot M 2009 *PhD Thesis* Technische Universiteit, Delft
[32] Nation P D, Blencowe M P and Buks E 2008 *Phys. Rev.* B **78** 104516
[33] Castellanos-Gomez A, Meerwaldt H B, Venstra W J, van der Zant H S J and Steele G A 2012 *Phys. Rev.* B **86** 041402
[34] Eichler A, del Álamo Ruiz M, Plza J A and Bachtold A 2012 *Phys. Rev. Lett.* **109** 025503